BMC Genomics

RESEARCH

Open Access

ATAC-seq and RNA-seq reveal key genes and pathways regulating lactation in the mammary gland of Yili horses

Lingling Liu[1*], Bin Chen[1], Mengjiao Kong[1], Yujie Tian[1], Haiyu Ma[1], Hang Cao[1] and Wujun Liu[1*]

Abstract

Background Mammary gland development and lactation are dynamic biological processes governed by coordinated changes in chromatin accessibility and gene expression.

Results We performed paired ATAC-seq and RNA-seq profiling to characterize stage-associated chromatin accessibility and transcriptional programs in the Yili horse mammary gland. Using a conservative overlap-based integration, we prioritized candidate genes showing concordant changes across both layers as hypothesis-generating signals for future functional studies. We sequenced mammary gland tissues from early lactation (S1) and peak lactation (S2) stages. We identified 32,187 S1-specific peaks and 46,661 S2-specific peaks. Upregulated genes were enriched in biological processes related to cell differentiation, tissue development, and signaling pathways, including PI3K-Akt, JAK-STAT, and Rap1 signaling, which may be involved in lactation regulation. In addition, motif enrichment analysis suggested several key transcription factors, including STAT5, SMAD4, and KLF3. Integration of ATAC-seq and RNA-seq data highlighted 22 differentially expressed genes (DEGs) with altered chromatin accessibility, including PTGES, NFATC4, RET, RGS2, and EQMHCB2, which are involved in the oxytocin signaling pathway, glutathione metabolism, and Wnt signaling.

Conclusions This study presents a stage-resolved atlas of chromatin accessibility and gene expression in the Yili horse mammary gland, suggesting candidate pathways and genes for further validation.

Keywords Yili horse, Mammary gland, ATAC-seq, RNA-seq, Regulatory genes

Background

Lactation is a fundamental physiological process in mammals that ensures neonatal nutrition, immune protection, and growth. In livestock, milk yield and composition directly affect both animal productivity and the dairy industry, with profound implications for food security and agricultural sustainability [1–3]. Milk synthesis and secretion are tightly regulated by the mammary gland, which undergoes dynamic structural and functional changes during pregnancy and lactation under the influence of hormones such as prolactin, estrogen, and glucocorticoids [4–6]. Perturbations in these regulatory

*Correspondence:
Lingling Liu
linglingliu1988@xjau.edu.cn
Wujun Liu
wujunliu1026@xjau.edu.cn
[1]College of Animal Science, Xinjiang Agricultural University, Urumqi 830052, China

networks may compromise milk production and animal health.

Advances in high-throughput technologies have provided new opportunities to dissect the molecular mechanisms underlying lactation. Transcriptome profiling (RNA-seq) has revealed stage-specific gene expression and non-coding RNA regulation, while chromatin accessibility assays (ATAC-seq) have identified cis-regulatory elements and transcription factor networks involved in mammary gland development [7, 8]. Integrated multi-omics approaches have been widely applied in livestock species such as cattle, pigs, and chickens, highlighting genetic and epigenetic factors that influence lactation performance [9–12].

By contrast, studies on equine lactation remain limited. Recent transcriptomic analyses in Kazakh horses have investigated the regulation of mammary gene expression across lactation stages [13, 14], and proteomic studies have described dynamic changes in equine milk proteins [15]. However, to date, no studies have applied chromatin accessibility profiling to investigate regulatory mechanisms in the equine mammary gland.

In this study, we performed parallel ATAC-seq and RNA-seq analyses of mammary tissues collected from Yili horses at early and peak lactation stages. By integrating transcriptomic and epigenomic data, we aimed to identify transcription factors and candidate genes involved in mammary development and milk synthesis. Our findings provide novel insights into the molecular regulation of equine lactation and a valuable resource for future functional and breeding studies.

Animals and sample collection

Six clinically healthy lactating, non-pregnant Yili mares (8 years old) were selected from a farm in Zhaosu County, Yili Kazakh Autonomous Prefecture, Xinjiang, China. Based on lactation stage, the animals were assigned to two groups: three mares in early lactation (month 1; M1-M3; group S1) and three mares in peak lactation (month 3; M4-M6; group S2). None of the mares had been bred prior to sampling, and pregnancy was therefore excluded at the time of tissue collection. All animals were maintained under standardized feeding and management conditions to minimize environmental variation. Following humane slaughter at the same abattoir, mammary gland tissue samples were collected from the same anatomical region in each mare to ensure sample consistency. Samples were immediately placed into sterile, RNase-free Eppendorf tubes, snap-frozen in liquid nitrogen, and transported to the laboratory for subsequent ATAC-seq and RNA-seq analyses.

Total RNA extraction, library construction, and sequencing

Total RNA was extracted from each sample using TRIzol reagent according to the manufacturer's instructions. RNA integrity and concentration were assessed using a Qsep400 system to ensure high-quality input material. For library preparation, 1 μg of total RNA was processed using the VAHTS Universal V10 Library Prep Kit for Illumina (NR606, Vazyme) [16]. Library construction comprised poly(A) + RNA selection, controlled RNA fragmentation, first-strand cDNA synthesis using random hexamers, second-strand cDNA synthesis, and PCR amplification. The resulting libraries were sequenced on the Illumina NovaSeq 6000 platform, producing 150 bp paired-end reads.

ATAC-seq library preparation and sequencing

ATAC-seq was performed by Edson Biotechnology Co., Ltd. (Xinjiang, China) as previously described [17]. Approximately 100 mg of mammary gland tissue was collected and immediately homogenized in 2 mL pre-chilled lysis buffer (15 mM Tris-HCl, pH 7.5; 20 mM NaCl; 80 mM KCl; 0.5 mM spermidine; 5 mM β-mercaptoethanol; 0.2% Triton X-100). The homogenate was filtered twice through Miracloth and layered onto 2 mL of dense sucrose buffer (20 mM Tris-HCl, pH 8.0; 2 mM $MgCl_2$; 2 mM EDTA; 15 mM β-mercaptoethanol; 1.7 M sucrose; 0.2% Triton X-100) in a 10 mL Falcon tube. Nuclei were pelleted by centrifugation at 2200 × g for 15 min at 4 °C and resuspended in 500 μL of pre-chilled lysis buffer.

For transposition, 25 μL reaction buffer, 2.5 μL Nextera Tn5 transposase, and 22.5 μL nuclease-free water were combined. Crude nuclei were incubated with the transposition mixture at 37 °C for 30 min. Transposed DNA was purified using the Qiagen MinElute PCR Purification Kit. Libraries were amplified using NEBNext High-Fidelity 2× PCR Master Mix for 10–15 cycles [18], subsequently purified with the MinElute kit, and eluted in 20 μL of elution buffer (10 mM Tris-HCl, pH 8). Library quality was assessed using a Bioanalyzer and Qubit, and qualified libraries were pooled and sequenced on an Illumina NovaSeq 6000 platform (paired-end 150 bp).

Bioinformatics analysis of RNA-seq

Adapter sequences and low-quality bases were trimmed with Cutadapt (v1.11), and high-quality reads were mapped to the EquCab3.0 reference genome using HISAT2 (v2.1.0), allowing up to two mismatches [19]. Gene annotation was performed based on the EquCab3.0 genome annotation, with functional annotation supported by the NCBI non-redundant (NR) protein database. Read counts were generated using FeatureCounts (v1.6.0) and normalized to Fragments Per Kilobase of transcript per Million mapped reads (FPKM) [20]. Differential expression analysis was performed using

Table 1 ATAC-seq data statistics

Sample	RawReads	RawBases	CleanReads	CleanBases	CleanRatio	Q20	Q30	GC
M1_RXL	101,097,400	15,164,610,000	100,962,750	10,378,570,064	99.87%	98.00%	93.35%	50.19%
M2_RXL	96,998,154	14,549,723,100	96,781,172	10,716,049,376	99.78%	97.84%	93.11%	49.35%
M3_RXL	101,695,756	15,254,363,400	101,501,998	9,554,390,238	99.81%	98.55%	94.99%	50.44%
M4_RXL	101,716,514	15,257,477,100	101,634,384	10,342,884,254	99.92%	97.23%	91.02%	51.46%
M5_RXL	100,166,260	15,024,939,000	100,012,328	9,574,133,758	99.85%	98.54%	95.02%	52.03%
M6_RXL	101,411,918	15,211,787,700	101,286,666	9,224,630,328	99.88%	98.33%	94.35%	50.72%

Table 2 Reference gene matching results

Group	sample	totalReads	mappedReads	mapRate	uniq	paired
S1	M1_RXL	100,962,750	84,528,120	83.72%	76,002,117	73,276,672
	M2_RXL	96,781,172	80,604,366	83.29%	74,739,967	72,178,976
	M3_RXL	101,501,998	82,217,123	81.00%	74,053,632	71,656,338
S2	M4_RXL	101,634,384	82,249,942	80.93%	75,498,965	72,147,538
	M5_RXL	100,012,328	81,913,581	81.90%	75,394,143	73,048,426
	M6_RXL	101,286,666	80,943,537	79.92%	74,493,290	72,086,800

edgeR, with significance defined as $p < 0.05$ and $|\log_2$ fold change$| > 1$. Functional enrichment of DEGs was assessed with clusterProfiler in R [21], and Gene Ontology (GO) [22] and Kyoto Encyclopedia of Genes and Genomes (KEGG) pathway enrichment was evaluated using a hypergeometric test, considering terms with $p < 0.05$ as significantly enriched [23].

ATAC-seq data analysis

Adapter sequences and low-quality reads were removed using Trimmomatic (v0.36). Clean reads were aligned to the EquCab3.0 reference genome using HISAT2 (v2.1.0), allowing up to two mismatches [24]. PCR duplicates were removed using SAMtools (v1.3.1). Peaks were identified using MACS2 (v2.1.1.20160309) with parameters: --nomodel, --shift – 100, --extsize 200, model fold = 5–50, and q-value < 0.05 [25]. Differential peaks were determined with DiffBind (v1.16.3) [26]. Peaks were assigned to genes if their midpoint was located within 5 kb upstream or downstream of the transcription start site (TSS). Functional enrichment analysis of associated genes was performed using clusterProfiler [21] in R for GO [22] and KEGG [23], with significance assessed using a hypergeometric test, with q < 0.05. Heatmaps depicting regulatory region distributions were generated using DeepTools (v3.2.1) [27], and motif enrichment was analyzed with HOMER (v3.0) using default settings and a maximum motif length of 12 bp [28].

Integration of ATAC-seq and RNA-seq

To generate hypotheses and prioritize candidates supported by two orthogonal layers, DEGs from RNA-seq were intersected with genes annotated to differential ATAC-seq peaks (± 5 kb around TSS). We defined genes with concordant direction of change in both datasets as "concordant candidates". This conservative integration is intended for candidate prioritization rather than mechanistic inference, because long-range enhancer–gene relationships cannot be resolved by proximity-based annotation alone. Genes showing consistent regulatory trends across both datasets were defined as candidate genes and were subsequently subjected to GO and KEGG enrichment analyses.

Results

Quality assessment of ATAC-seq data for Yili horse mammary tissues

To investigate regulatory mechanisms underlying differences between two stages, ATAC-seq was performed on the S1 and S2 groups to assess genome-wide chromatin accessibility. A total of 97–102 million raw reads were generated for each of the six samples. After quality control, more than 96 million clean reads were retained for each sample (Table 1). On average, 82.67% and 80.92% of clean reads from the S1 and S2 groups, respectively, were successfully mapped to the EquCab3.0 reference genome (Table 2). Library quality was evaluated based on insert fragment length and peak signal distribution. As shown in Fig. 1A, B, the non-redundant fraction (NRF), PCR bottleneck coefficient 1 (PBC1), and PCR bottleneck coefficient 2 (PBC2) were 0.99 ± 0.004, 0.99 ± 0.003, and 214.48 ± 100.66, respectively. NRF reflects the proportion of uniquely mapped reads, while PBC1 and PBC2 indicate library complexity. Thresholds of NRF > 0.9, PBC1 > 0.9, and PBC2 > 3 are typically considered acceptable. All values in this study exceeded these quality control criteria, demonstrating the high consistency and complexity of the sequencing libraries.

The fragment length distribution of the ATAC-seq data from all six samples (Fig. 1C) showed enrichment at approximately 100 bp, indicating that most insert fragments correspond to nucleosome-free regions. The

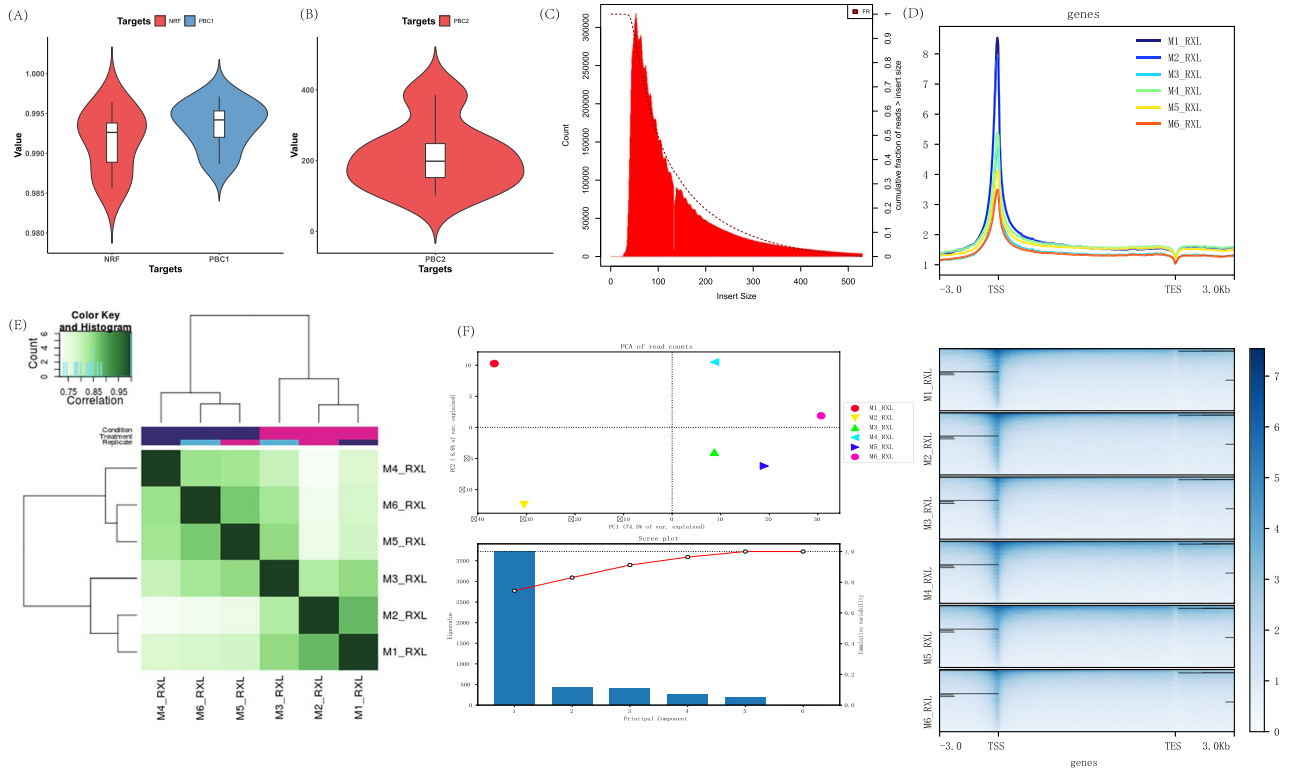

Fig. 1 Quality statistics of ATAC-seq in Yili horse mammary. **A**, **B** ATAC-seq sequencing quality statistics, where NRF represents the non-redundant fraction, calculated as NRF = number of uniquely aligned reads/total number of reads. PBC1 represents Phantom Peak Coefficient 1, calculated as PBC1 = number of uniquely aligned reads/number of reads aligned multiple times. PBC2 represents Phantom Peak Coefficient 2, calculated as PBC2 = number of singly aligned reads/total number of reads. **C** Statistics on the fragment size distribution of ATAC-seq libraries. The Insert Size represents the length of sequencing reads. FR (Forward-Reverse orientation) indicates the normal paired-end sequencing orientation. **D** ATAC-seq signal enrichment surrounding the TSS. The y-axis represents the degree of enrichment of all genes at the TSS (Transcription Start Site), with enrichment gradually decreasing from top to bottom. The x-axis represents the distance from the TSS, where negative values indicate upstream regions and positive values indicate downstream regions. **E** Clustering heatmap of accessible regions in Yili horse mammary. **F** PCA plot

majority of accessible chromatin regions were located within 3 kb of transcription start sites (TSSs), emphasizing their potential regulatory roles (Fig. 1D). Correlation heatmap analysis of peak signals revealed clear differences between the S1 and S2 groups, confirming the reproducibility of biological replicates (Fig. 1E). Principal component analysis (PCA) further supported this finding, showing a distinct separation between the two groups, with PC1 and PC2 explaining 74.5% and 8.6% of the total variance, respectively (Fig. 1F). Collectively, these results indicate that the ATAC-seq data are of sufficient quality for downstream analyses.

Chromatin accessibility in the mammary gland of Yili horses

A total of 32,187 peaks were uniquely identified in the S1 group, 46,661 peaks were specific to the S2 group, and 48,061 peaks were shared between both stages (Fig. 2A). The chromosomal distribution of these peaks is shown in Fig. 2B. Peaks were distributed across most chromosomes, including the X chromosome, whereas eight chromosomes exhibited no detectable peak enrichment. To characterize the functional genomic context of the accessible chromatin regions, all peaks were annotated using genomic reference files. The annotated regions were categorized into intergenic, other intron, first intron, promoter_0kb_1kb, other exon, first exon, promoter_1kb_2kb, 5′UTR, promoter_2kb_3kb, and 3′UTR elements (Fig. 2C). The majority of peaks were located within intergenic regions, first introns, and other regions. Notably, peaks located within promoter regions (0–1 kb upstream of the TSS) accounted for 3.37% of the total in S1 and 2.72% in S2 (Fig. 2D, E).

GO and KEGG analysis of genes associated with differential peaks and motif enrichment analysis

To identify open chromatin regions associated with mammary gland development, stage-specific peaks were annotated, resulting in 2,509 associated genes, including 193 genes associated with peaks showing increased accessibility and 2,316 genes associated with peaks showing decreased accessibility. To investigate the biological functions of these genes, GO and KEGG pathway enrichment analyses were performed. For genes associated

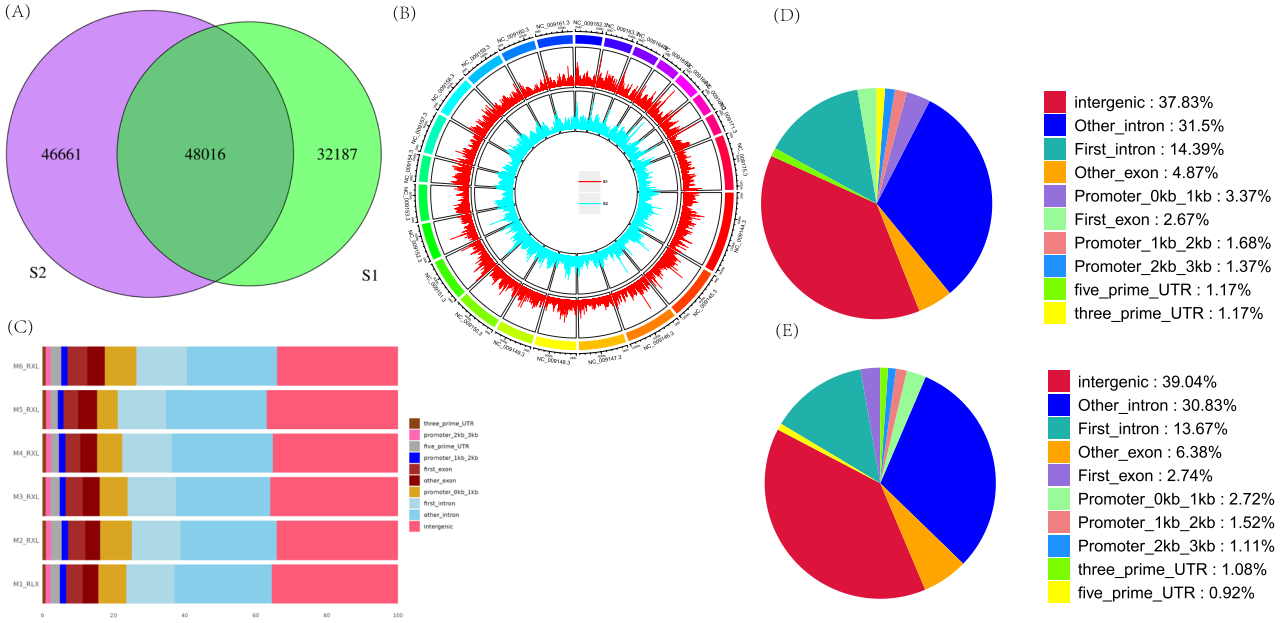

Fig. 2 Identification and analysis of peaks. **A** Venn diagram illustrates peak overlap between S1 and S2. **B** Chromosomal distribution of all peaks. **C** Distribution ratio of peaks in gene functional elements. **D** Distribution of S1-special peaks in gene functional elements. **E** Distribution of S2-special peaks in gene functional elements

with decreased accessibility, GO terms were significantly enriched in female pregnancy, vasculogenesis, immune system processes, and signaling receptor or cytokine binding (Fig. 3A, Table S1[see Additional file 1]). A total of 54 KEGG pathways were significantly enriched ($p < 0.05$), many of which were associated with metabolic processes and cellular signal transduction (Fig. 3B, Table S2[see Additional file 2]).

For genes associated with increased chromatin accessibility, enriched GO terms were mainly related to cell differentiation, tissue development, regulation of multicellular organismal processes, and signaling receptor binding (Fig. 3C, Table S3[see Additional file 3]). Thirty-nine KEGG pathways were significantly enriched ($p < 0.05$), many of which were associated with the PI3K-Akt, JAK-STAT, and Rap1 signaling pathways (Fig. 3D, Table S4[see Additional file 4]). These pathways are known to be associated with lactation, indicating that chromatin accessibility changes during peak lactation may influence milk production–related signaling.

To identify key transcription factors (TFs) potentially regulating chromatin accessibility, de novo motif enrichment analysis was conducted on the differential ATAC-seq peaks. Motif enrichment analysis of differential ATAC-seq peaks was performed using HOMER software. The top 10 transcription factor binding motifs enriched in peaks with increased accessibility included RBM28, KLF1, PITX1, MET31, and SOX2 (Fig. 3E). In contrast, motifs enriched in peaks with reduced accessibility were primarily associated with the STAT and ETS transcription factor families (Fig. 3F).

RNA-seq data from mammary tissues of Yili horses

High-quality RNA was obtained from all mammary tissue samples, as indicated by quality control metrics (Table S5 [see Additional file 5]). More than 98% of clean reads were successfully mapped to the EquCab 3.0 reference genome. The majority of reads aligned to coding sequence (CDS) regions in all six samples, indicating high data reliability (Fig. S1 [see Additional file 6]).

In total, 393 DEGs were identified between the two groups, including 326 upregulated and 67 downregulated genes. GO and KEGG pathway enrichment analyses were performed separately for upregulated and downregulated mRNAs. The DEGs were enriched in GO terms mainly related to immune response, inflammatory regulation, cytokine signaling, and extracellular matrix (ECM) organization and function, including extracellular matrix organization and extracellular structure organization. These processes are involved in ECM remodeling and play critical roles in mammary branching morphogenesis and epithelial cell differentiation (Fig. 4A, Table S6 [see Additional file 7]). Additionally, 23 KEGG pathways were significantly enriched (adjusted $p < 0.05$). Many of these pathways are associated with mammary gland development and lactation, particularly the PI3K-Akt and Rap1 signaling pathways (Fig. 4B).

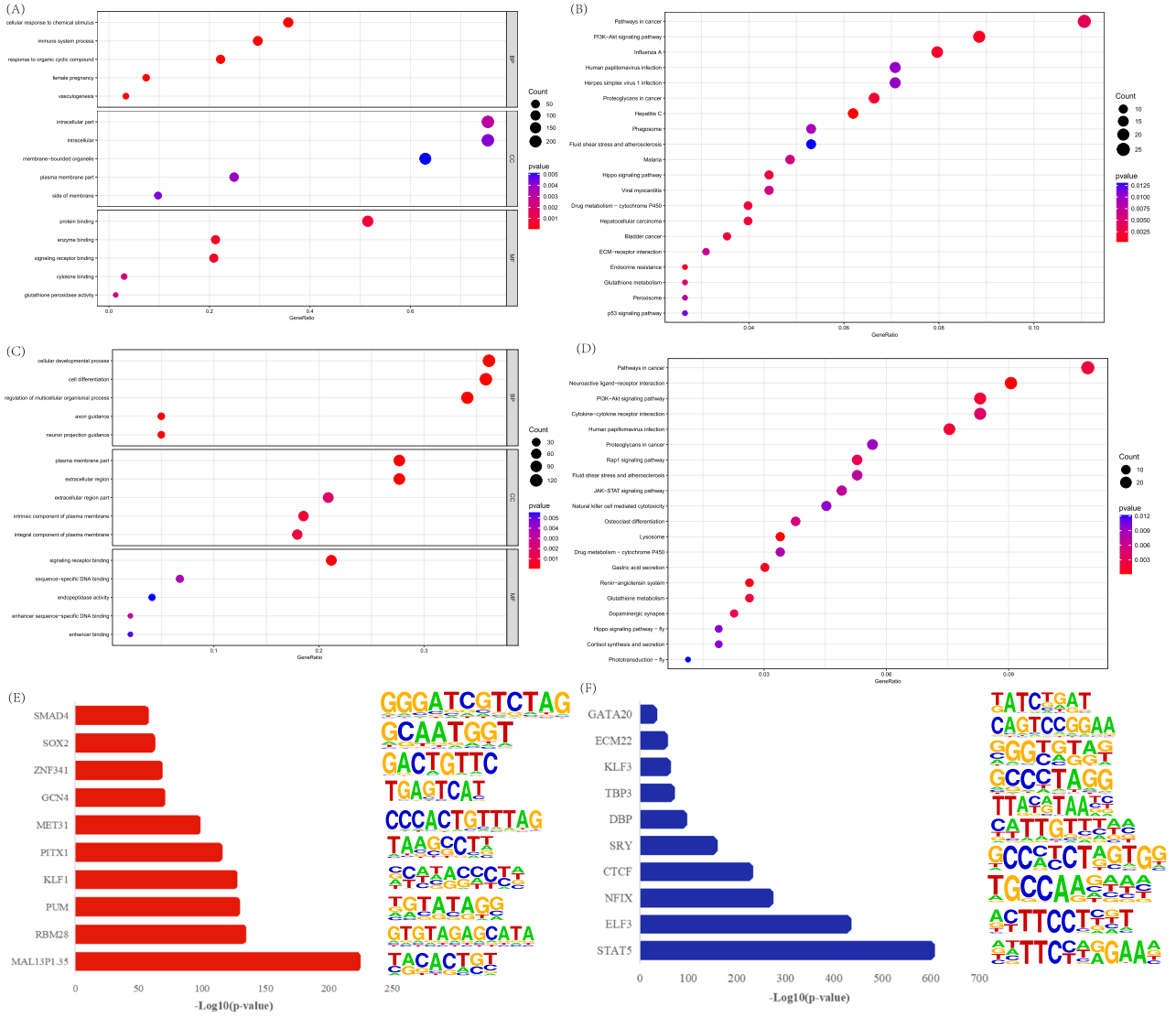

Fig. 3 Enrichment analysis of genes associated with differential peaks. **A** GO enrichment analysis of down-regulated genes. **B** GO enrichment analysis of up-regulated genes. **C** KEGG enrichment analysis of down-regulated genes. **D** KEGG enrichment analysis of up-regulated genes. **E**, **F** The top 10 transcription factor binding motifs were enriched in significantly higher and significantly lower peak areas based on the p-values between the two groups, respectively

Integration analysis of ATAC-seq and RNA-seq

To explore cross-layer concordance between chromatin accessibility and transcription, we intersected DEGs with genes annotated to differential ATAC-seq peaks. This integrative analysis identified 22 DEGs showing concordant changes in both chromatin accessibility and transcription, including 16 downregulated and 6 upregulated genes (Fig. 5A, B; Table 3). Functional enrichment analysis showed that these DEGs were enriched in biological processes related to enzyme activity, cell growth, chromatin binding, and the calcineurin–NFAT signaling pathway (Fig. 5C, E). Among these DEGs, PTGES, NFATC4, RET, RGS2, and EQMHCB2 were highlighted as candidate genes of interest. KEGG enrichment analysis indicated that these genes were involved in the oxytocin signaling pathway, glutathione metabolism, and Wnt signaling (Fig. 5D, F; Table S7[see Additional file 8]).

Discussion

Milk yield, which is largely determined by mammary gland development, is a key factor in evaluating the economic value of livestock [29]. Understanding the molecular mechanisms underlying mammary gland development is therefore essential for the selective breeding of high-yield dairy horses and for improving production efficiency. In recent years, studies in horses have mainly relied on approaches such as single-cell RNA sequencing and chromatin immunoprecipitation

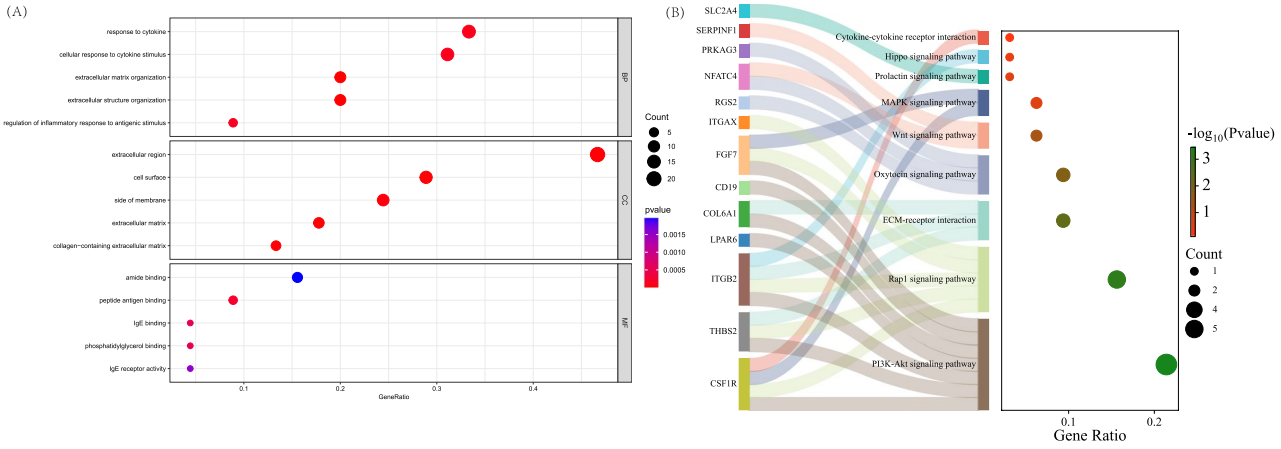

Fig. 4 Identification of differentially expressed genes in the mammary gland of Yili horses. **A** GO enrichment of differentially expressed genes. **B** KEGG signaling pathways related to mammary gland development identified from DEGs. The Sankey diagram on the left displays the enriched pathways corresponding to key candidate genes

sequencing [30]. However, investigations of equine traits from the perspective of chromatin accessibility remain limited [31]. To address this gap, we profiled chromatin accessibility at two stages and integrated these data with transcriptomic profiles. Furthermore, we integrated ATAC-seq and RNA-seq data to highlight candidate regulators that may contribute to mammary gland development in Yili horses.

RNA-seq provides reliable tissue-level expression profiles that reflect downstream transcriptional outputs, whereas ATAC-seq profiles chromatin accessibility and provides regulatory context that can help link genomic variation to transcriptional regulation [32]. Increasing evidence suggests that integrating RNA-seq with chromatin accessibility data improves biological interpretation and the accuracy of candidate gene prioritization. For instance, Zhang et al. combined endometrial ATAC-seq and RNA-seq to pinpoint candidate genes associated with reproductive performance, including ANXA4 [9]. More broadly, multi-omics studies indicate that expression divergence can occur even when global accessibility patterns appear relatively stable, because allele-specific expression is largely explained by allele-specific DNA methylation and chromatin accessibility [33]. Taken together, these findings support the necessity of performing both ATAC-seq and RNA-seq in parallel: RNA-seq delineates lactation stage–associated transcriptional programs, while ATAC-seq provides the regulatory landscape that facilitates mechanistic interpretation and prioritization of candidate genes and pathways for downstream validation.

Chromatin accessibility is a key determinant of gene regulation and is closely associated with gene expression. Active genes and regulatory elements are typically located within or adjacent to DNA regions that are accessible to transcription factors. Thus, identifying open chromatin regions is important for characterizing tissue-specific regulatory elements and for advancing the understanding of complex traits in horses [31]. ATAC-seq is widely used to detect such open chromatin regions [7]. In this study, ATAC-seq peaks were enriched near transcription start sites (TSSs) in both the S1 and S2 groups, supporting their potential roles as regulatory hubs for transcription factor binding. In both groups, a large proportion of peaks was located in intergenic regions and introns, with intergenic regions accounting for 38.43% on average and other introns accounting for 31.17%. These were followed by peaks located in the first intron, exons, and promoter regions. Notably, promoter-associated peaks accounted for 5.88% on average, which is higher than the 4.3% reported in bovine mammary tissue [34], but lower than values reported in pigs, where promoter peaks within 3 kb accounted for 31.31% ± 4.47% [35]. These interspecies differences may reflect differences in genome annotation, peak-calling definitions, tissue composition, and species-specific regulatory architectures.

We next compared chromatin accessibility between two groups. ATAC-seq identified 46,661 peaks with increased accessibility and 32,187 peaks with decreased accessibility. Functional enrichment analysis of genes annotated to these differential peaks indicated enrichment in pathways related to signal transduction, metabolism, and tissue processes, including PI3K–Akt signaling. Previous studies in bovine cells have shown that PI3K/Akt/mTORC1 can activate MMP9 through NF-κB and thereby contribute to mammary gland remodeling [36]. In ZEA-induced mouse and cell models, NAC was reported to reverse ROS-mediated inhibition of this pathway, supporting a role of PI3K-Akt signaling in maintaining lactation capacity [37]. Consistent with this, PI3K-Akt signaling has also been implicated in regulating milk fat synthesis in mammary epithelial cells [38]. In addition, motif

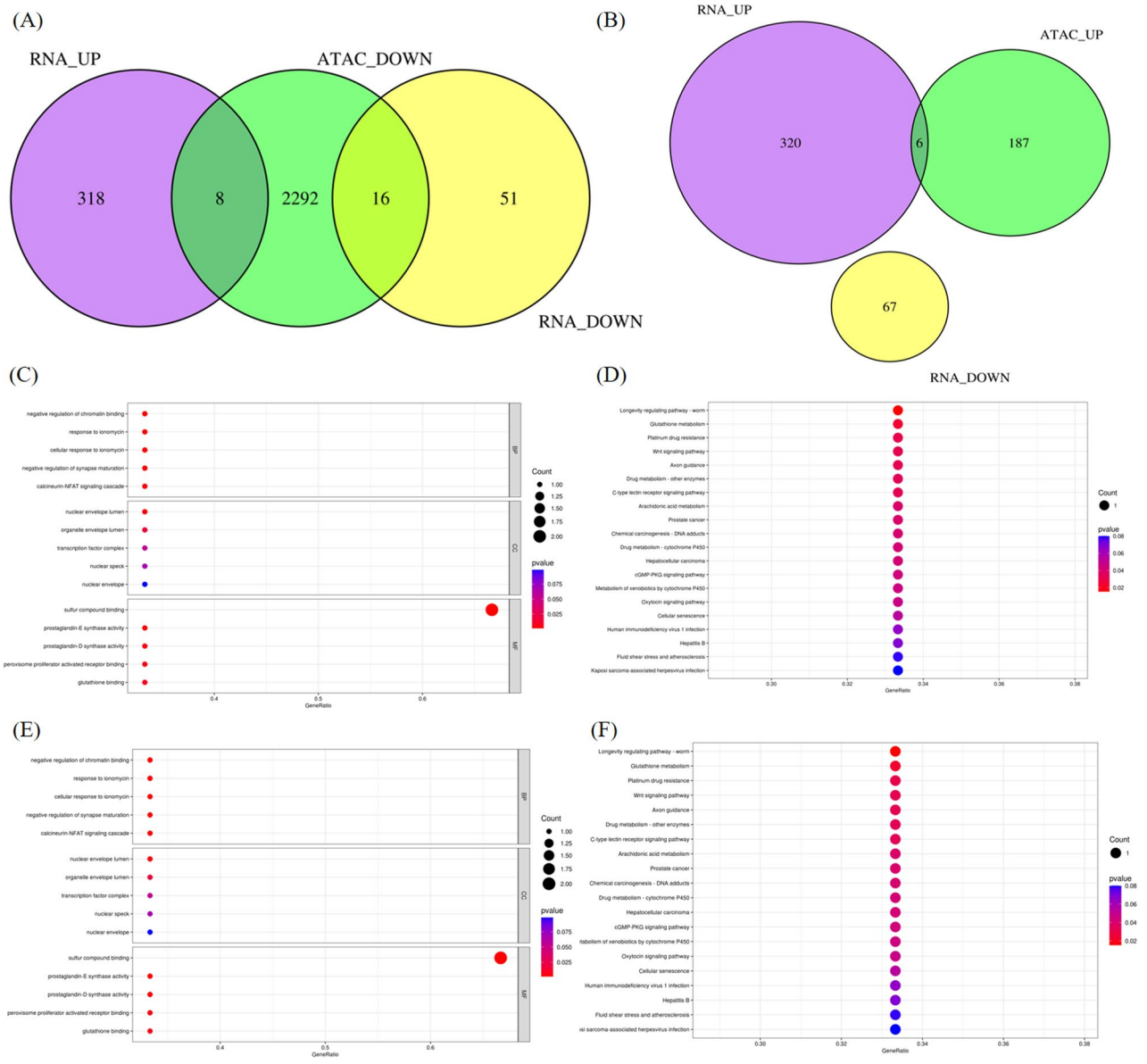

Fig. 5 Integration of data from ATAC-seq and RNA-seq. **A** Overlap with the downregulated genes. **B** Overlap with the upregulated genes. **C** GO enrichment analysis of differentially upregulated genes. **D** KEGG pathway of differentially upregulated genes. **E** GO enrichment analysis of differentially downregulated genes. **F** KEGG pathway of differentially downregulated genes

Table 3 Chromatin accessibility of diferentially expressed genes

	Upregulated Gene Number	Downregulated Gene Number	Total
ATAC-seq	193	2316	2509
RNA-seq	326	67	393
Overlap	6	16	22

enrichment analysis suggested potential involvement of transcription factors such as STAT5, SMAD4, CTCF, and ELF3 in mammary gland development. Knockout studies have shown that STAT5 deficiency does not impair normal development but disrupts mammary lobuloalveolar outgrowth during pregnancy, resulting in lactation failure due to impaired terminal differentiation, supporting its central role in mammopoietic and lactogenic signaling [39]. Another enriched pathway, JAK-STAT signaling, particularly involving STAT5a and STAT5b, is known to regulate mammary-specific gene expression during pregnancy and lactation [40]. STAT5a primarily regulates alveolar formation and milk synthesis, whereas STAT5b promotes ductal growth and branching. Both have been reported to be important for mammary development [41]. During mid-pregnancy, RANK signaling promotes precursor cell expansion and alveolar generation, but may also inhibit prolactin activity by interfering with STAT5 activation [42]. Collectively, these pathways and

their interactions with hormones and growth factors are likely to contribute to mammary gland maturation and function. SMAD4, a central mediator of canonical transforming growth factor-beta (TGF-β) signaling, plays an important role in cell fate determination in multicellular organisms [43]. SMAD4 forms complexes with receptor-regulated SMADs (R-SMADs), including SMAD2, SMAD3, and SMAD1/5, thereby enabling diverse SMAD complexes downstream of BMP or TGF-β signaling. These complexes can bind TGF-β–responsive elements, typically CAGA motifs, thereby influencing cell proliferation, differentiation, and tissue remodeling [44–46]. CTCF establishes regulatory boundaries between genes and can influence enhancer activity in a context-dependent manner. CTCF contributes to genome topology, domain boundary formation, and long-range chromatin interactions. In the mammary gland, CTCF binding sites have been implicated in promoter–enhancer interactions of highly expressed genes, such as caseins. Disruption of these sites has been reported to alter mammary gene expression [47, 48]. Epithelium-specific ETS (ESE) transcription factors, a subgroup of the ETS family, have been reported to play roles in epithelial development, differentiation, and homeostasis. ELF3 is upregulated in the mammary epithelium of mice during pregnancy and early lactation and has been reported to regulate milk protein genes such as WAP while maintaining epithelial identity [49].

A total of 22 DEGs were identified with concordant evidence from both datasets. Functional enrichment analysis indicated that these genes were enriched in the Wnt and oxytocin signaling pathways. Among these candidates, PTGES, NFATC4, RET, and RGS2 were highlighted due to potential relevance to mammary gland development and lactation in Yili horses. PTGES participates in PGE_2 synthesis, and PGE_2 has been implicated in regulating inflammation and angiogenesis in mammary tissue, potentially shaping the mammary microenvironment via aromatase-related mechanisms. PGE_2 levels vary across development and lactation, and genetic deletion of mPGES-1 has been shown to reduce mammary PGE_2 and affect angiogenesis and tissue phenotypes, supporting PTGES as a candidate regulator in Yili horses [50–52]. The NFAT family of transcription factors, activated by the calmodulin/calcineurin pathway, has been implicated in regulating cell differentiation, proliferation, angiogenesis, and inflammation. Calcineurin–NFAT signaling has been reported to be active in mammary morphogenesis and stromal–vascular interactions and is also implicated in tumor biology. NFAT family members such as NFATc1, NFATc3, and NFATC4 have been implicated in mammary development, and NFATc1 has been reported to play roles in mammary morphogenesis and stem cell differentiation. NFATC4 has been studied in breast cancer contexts and has been reported to influence proliferation and migration, suggesting potential roles in mammary epithelial cell fate determination and transcriptional regulation [53–55]. RGS2 has been reported to be highly expressed in mammary myoepithelial and basal cells. Functional studies have shown that it can modulate oxytocin receptor (OXTR) signaling, thereby influencing the contractile response of myoepithelial cells. Because oxytocin-induced myoepithelial contraction is essential for milk ejection, RGS2 may influence lactation physiology by modulating OXTR signaling [56, 57]. RET has been reported to be highly expressed in the mammary gland during lactation and to decline during weaning and involution. Persistent RET expression during lactation has been reported to activate STAT3-associated inflammatory pathways and to disrupt tissue remodeling [58, 59]. In summary, these genes and pathways represent candidate regulators of mammary gland development and lactation. Motif enrichment and pathway analyses highlighted TF families and signaling pathways previously implicated in mammary development and lactation in other species. In the absence of long-range regulatory mapping and functional perturbation, these results should be interpreted as hypothesis-generating associations rather than causal mechanisms. Nevertheless, the concordant candidates (e.g., PTGES, NFATC4, RET, RGS2) provide a focused shortlist for future validation in equine mammary biology.

Limitations

The main limitation of this study is the small sample size ($n = 3$ mares per lactation stage), largely due to the practical constraints of obtaining mammary tissue in large livestock, which typically requires slaughter. Our multi-omics integration has inherent limitations. Proximity-based peak-to-gene annotation cannot resolve distal enhancer–gene relationships, and without temporal/perturbation or 3D genome evidence, regulatory directionality and causal inference remain unclear. Therefore, the enriched TF motifs, associated pathways, and concordant ATAC–RNA candidates reported here may serve as valuable starting points for hypothesis generation and candidate prioritization. Future studies with larger cohorts, additional lactation time points, and independent populations are needed to validate the identified regulatory elements, pathways, and candidate genes, together with functional validation (e.g., qPCR and targeted assays).

Conclusions

This study provides an initial (first-pass) chromatin accessibility map and transcriptomic profile of the Yili horse mammary gland across early and peak lactation stages. This study presents the first chromatin accessibility map of Yili horse mammary tissue, revealing regions

of accessible chromatin. In addition, the genes identified by RNA-seq exhibited distinct transcriptional patterns between the two stages. By integrating the results from both approaches, we identified five key candidate genes potentially involved in mammary gland development.

Abbreviations

DEGs	Differentially Expressed Genes
EQMHCB2	MHC class II beta 2
GO	Gene Ontology
KEGG	Kyoto Encyclopedia of Genes and Genomes
KLF1	KLF Transcription Factor 1
KLF3	KLF Transcription Factor 3
MET31	Zinc-finger DNA-binding protein MET31
NFATC4	Nuclear Factor of Activated T Cells 4
NRF	The non-redundant fraction
PBC1	PCR bottleneck coefficient 1
PBC2	PCR bottleneck coefficient 2
PCA	Principal component analysis
PITX1	Paired Like Homeodomain 1
PTGES	Prostaglandin E Synthase
RBM28	RNA Binding Motif Protein 28
RET	Ret Proto-Oncogene
RGS2	Regulator of G Protein Signaling 2
SMAD4	SMAD Family Member 4
SOX2	SRY-Box Transcription Factor 2
STAT5	Signal Transducer and Activator of Transcription 5 A
TFs	Transcription Factors

Supplementary Information

The online version contains supplementary material available at https://doi.org/10.1186/s12864-026-12840-6.

Additional file 1: Table S1. GO enrichment terms for ATAC-seq downregulated genes. Description: This table lists the GO enrichment analysis results for genes associated with downregulated genes in Yili horse mammary gland, including GO terms, p-values, gene ID, and gene counts.

Additional file 2: Table S2. KEGG enriched pathways for ATAC-seq downregulated genes. Description: This table presents KEGG pathway enrichment analysis for genes linked to downregulated ATAC-seq peaks, showing pathway names, p-values, adjusted p-values, and associated gene lists in Yili horse.

Additional file 3: Table S3. GO enrichment terms for ATAC-seq upregulated genes. Description: This table summarizes GO enrichment results for genes associated with upregulated ATAC-seq peaks in Yili horse mammary gland, with details on biological processes, p-values, and enriched gene numbers.

Additional file 4: Table S4. KEGG enriched pathways for ATAC-seq upregulated genes. Description: This table details KEGG pathway enrichment for genes from upregulated ATAC-seq peaks, including pathway IDs, descriptions, p-value, and gene ID, and gene counts.

Additional file 5: Table S5. RNA-seq read mapping statistics. Description: This table provides quality control metrics for RNA-seq data mapping in Yili horse mammary gland samples, including total reads, mapped reads, and mapping rates.

Additional file 6: Fig. S1. Genomic distribution of reads.

Additional file 7: Table S6. GO enrichment terms for RNA-seq differentially expressed genes. Description: This table reports GO enrichment analysis for differentially expressed genes identified from RNA-seq in lactating Yili horse mammary gland.

Additional file 8: Table S7. KEGG pathways for shared differentially expressed genes from ATAC-seq and RNA-seq integration. Description: This table shows KEGG enrichment results for overlapping differentially expressed genes from integrated ATAC-seq and RNA-seq analyses, highlighting key lactation-related pathways with gene overlaps and statistical significance.

Acknowledgements
The authors would like to express sincere gratitude to Chunsheng Shao for his valuable encouragement during the preparation of this manuscript.

Authors' contributions
L.L. and W.L. contributed to the conception, design, and planning of the study. C.B., M.K., and Y.T. acquired the data. L.L., H.M., H.C. contributed to the interpretation of the results. L.L. drafted the manuscript. L.L., H.C. collaborated on the manuscript tables and figures. All authors contributed to the drafting or critical review of the manuscript and all authors had access to the data, which was verified by L.L. and W.L.

Funding
This research was funded by Tianshan Talent Program, grant number 2023TSYCCX0033.

Data availability
The datasets generated and/or analyzed during the current study are available in the CNCB-NGDC repository under the following accession numbers: horse RNA-sequencing data: https://ngdc.cncb.ac.cn/gsa/s/N29E10V2 (CRA031374), horse ATAC data: https://ngdc.cncb.ac.cn/gsa/s/uiyTaduE (CRA031160).

Declarations

Ethics approval and consent to participate
This study aimed to investigate mammary gland tissues in horses, and the use of animals was justified by the lack of viable alternatives and minimized in accordance with the 3R principles. all mares were rendered unconscious by electrical stunning in accordance with the Chinese National Standard SN/T 4102 – 2015 "Animal welfare specification for horses during breeding, transport and slaughter". Immediately after stunning, exsanguination was performed via severance of the carotid arteries and jugular veins, and death was confirmed prior to tissue collection. The protocol, involving the slaughter of six horses for tissue collection, was reviewed and approved by the animal welfare and ethics Committee of Xinjiang agricultural university (Approval No. 2024044).

Consent for publication
Not applicable.

Competing interests
The authors declare no competing interests.

Received: 6 October 2025 / Accepted: 2 April 2026
Published online: 22 April 2026

References

1. Hue-Beauvais C, Faulconnier Y, Charlier M, Leroux C. Nutritional Regulation of Mammary Gland Development and Milk Synthesis in Animal Models and Dairy Species. Genes (Basel). 2021;12:523. https://doi.org/10.3390/genes12040523.
2. Qasba PK, Dandekar AM, Horn TM, Losonczy I, Siegel M, Sobiech KA, et al. Milk protein gene expression in the rat mammary gland. Crit Rev Food Sci Nutr. 1982;16:165–86. https://doi.org/10.1080/10408398209527332.
3. Brisken C, Hess K, Jeitziner R. Progesterone and Overlooked Endocrine Pathways in Breast Cancer Pathogenesis. Endocrinology. 2015;156:3442–50. https://doi.org/10.1210/en.2015-1392.
4. Macias H, Hinck L. Mammary gland development. Wiley Interdiscip Rev Dev Biol. 2012;1:533–57. https://doi.org/10.1002/wdev.35.
5. Canul-Medina G, Fernandez-Mejia C. Morphological, hormonal, and molecular changes in different maternal tissues during lactation and post-lactation. J Physiol Sci. 2019;69:825–35. https://doi.org/10.1007/s12576-019-00714-4.
6. Neville MC, McFadden TB, Forsyth I. Hormonal regulation of mammary differentiation and milk secretion. J Mammary Gland Biol Neoplasia. 2002;7:49–66. https://doi.org/10.1023/a:1015770423167.

7. Buenrostro JD, Wu B, Chang HY, Greenleaf WJ. ATAC-seq: A Method for Assaying Chromatin Accessibility Genome-Wide. Curr Protoc Mol Biol. 2015;109:21.29.1-21.29.9. https://doi.org/10.1002/0471142727.mb2129s109.
8. Corces MR, Trevino AE, Hamilton EG, Greenside PG, Sinnott-Armstrong NA, Vesuna S, et al. An improved ATAC-seq protocol reduces background and enables interrogation of frozen tissues. Nat Methods. 2017;14:959–62. https://doi.org/10.1038/nmeth.4396.
9. Zhang H, Liu Z, Wang J, Zeng T, Ai X, Wu K. An Integrative ATAC-Seq and RNA-Seq Analysis of the Endometrial Tissues of Meishan and Duroc Pigs. Int J Mol Sci. 2023;24:14812. https://doi.org/10.3390/ijms241914812.
10. Zhao Z, Guo D, Wei Y, Li J, Jia X, Niu Y, et al. Integrative ATAC-seq and RNA-seq Analysis of the Longissimus Dorsi Muscle of Gannan Yak and Jeryak. Int J Mol Sci. 2024;25:6029. https://doi.org/10.3390/ijms25116029.
11. Zheng W, Zhang J, Huang J, Han B, Liu Y, Sun D. A pilot multi-omics study reveals genetic mechanisms regulating milk component traits in dairy cattle. Commun Biol. 2025;8:1150. https://doi.org/10.1038/s42003-025-08615-6.
12. Zhang X, Li J, Wang X, Jie Y, Sun C, Zheng J, et al. ATAC-seq and RNA-seq analysis unravel the mechanism of sex differentiation and infertility in sex reversal chicken. Epigenetics Chromatin. 2023;16:2. https://doi.org/10.1186/s13072-022-00476-1.
13. Yu X, Fang C, Liu L, Zhao X, Liu W, Cao H, et al. Transcriptome study underling difference of milk yield during peak lactation of Kazakh horse. J Equine Vet Sci. 2021;102:103424. https://doi.org/10.1016/j.jevs.2021.103424.
14. Zhang Z, Lu Z, Yao X, Li L, Meng J, Wang J, et al. Influence of Pregnancy on Whole-Transcriptome Sequencing in the Mammary Gland of Kazakh Mares. Anim (Basel). 2025;15:2056. https://doi.org/10.3390/ani15142056.
15. Blanco-Doval A, Azkargorta M, Iloro I, Beaskoetxea J, Elortza F, Barron LJR, et al. Comparative proteomic analysis of the changes in mare milk associated with different lactation stages and management systems. Food Chem. 2024;445:138766. https://doi.org/10.1016/j.foodchem.2024.138766.
16. Xu L, Li S, Shabala S, Jian T, Zhang W. Plants Grown in Parafilm-Wrapped Petri Dishes Are Stressed and Possess Altered Gene Expression Profile. Front Plant Sci. 2019;10:637. https://doi.org/10.3389/fpls.2019.00637.
17. Wu J, Huang B, Chen H, Yin Q, Liu Y, Xiang Y, et al. The landscape of accessible chromatin in mammalian preimplantation embryos. Nature. 2016;534:652–7. https://doi.org/10.1038/nature18606.
18. Lu Z, Hofmeister BT, Vollmers C, DuBois RM, Schmitz RJ. Combining ATAC-seq with nuclei sorting for discovery of cis-regulatory regions in plant genomes. Nucleic Acids Res. 2017;45:e41. https://doi.org/10.1093/nar/gkw1179.
19. Su W-L, Liu N, Mei L, Luo J, Zhu Y-J, Liang Z. Global Transcriptomic Profile Analysis of Genes Involved in Lignin Biosynthesis and Accumulation Induced by Boron Deficiency in Poplar Roots. Biomolecules. 2019;9:156. https://doi.org/10.3390/biom9040156.
20. Li B, Dewey CN. RSEM: accurate transcript quantification from RNA-Seq data with or without a reference genome. BMC Bioinformatics. 2011;12:323. https://doi.org/10.1186/1471-2105-12-323.
21. Yu G, Wang L-G, Han Y, He Q-Y. clusterProfiler: an R Package for Comparing Biological Themes Among Gene Clusters. OMICS. 2012;16:284–7. https://doi.org/10.1089/omi.2011.0118.
22. Ashburner M, Ball CA, Blake JA, Botstein D, Butler H, Cherry JM, et al. Gene Ontology: tool for the unification of biology. Nat Genet. 2000;25:25–9. https://doi.org/10.1038/75556.
23. Kanehisa M, Goto S. KEGG: kyoto encyclopedia of genes and genomes. Nucleic Acids Res. 2000;28:27–30. https://doi.org/10.1093/nar/28.1.27.
24. Keel BN, Snelling WM. Comparison of Burrows-Wheeler Transform-Based Mapping Algorithms Used in High-Throughput Whole-Genome Sequencing: Application to Illumina Data for Livestock Genomes. Front Genet. 2018;9:35. https://doi.org/10.3389/fgene.2018.00035.
25. Dong Z, Xiao Y, Govindarajulu R, Feil R, Siddoway ML, Nielsen T, et al. The regulatory landscape of a core maize domestication module controlling bud dormancy and growth repression. Nat Commun. 2019;10:3810. https://doi.org/10.1038/s41467-019-11774-w.
26. Robinson MD, Strbenac D, Stirzaker C, Statham AL, Song J, Speed TP, et al. Copy-number-aware differential analysis of quantitative DNA sequencing data. Genome Res. 2012;22:2489–96. https://doi.org/10.1101/gr.139055.112.
27. Iberg-Badeaux A, Collombet S, Laurent B, van Oevelen C, Chin K-K, Thieffry D, et al. A Transcription Factor Pulse Can Prime Chromatin for Heritable Transcriptional Memory. Mol Cell Biol. 2017;37:e00372–16. https://doi.org/10.1128/MCB.00372-16.
28. Heinz S, Benner C, Spann N, Bertolino E, Lin YC, Laslo P, et al. Simple combinations of lineage-determining transcription factors prime cis-regulatory elements required for macrophage and B cell identities. Mol Cell. 2010;38:576–89. https://doi.org/10.1016/j.molcel.2010.05.004.
29. Rowson AR, Daniels KM, Ellis SE, Hovey RC. Growth and development of the mammary glands of livestock: a veritable barnyard of opportunities. Semin Cell Dev Biol. 2012;23:557–66. https://doi.org/10.1016/j.semcdb.2012.03.018.
30. Barber AM, Kingsley NB, Peng S, Giulotto E, Bellone RR, Finno CJ, et al. Annotation of cis-regulatory-associated histone modifications in the genomes of two Thoroughbred stallions. Front Genet. 2025;16:1534461. https://doi.org/10.3389/fgene.2025.1534461.
31. Peng S, Bellone R, Petersen JL, Kalbfleisch TS, Finno CJ. Successful ATAC-seq from Snap-Frozen Equine tissues. Front Genet. 2021;12:641788. https://doi.org/10.3389/fgene.2021.641788.
32. Luo L, Gribskov M, Wang S. Bibliometric review of ATAC-seq and its application in gene expression. Brief Bioinform. 2022;23:bbac061. https://doi.org/10.1093/bib/bbac061.
33. Quan J, Yang M, Wang X, Cai G, Ding R, Zhuang Z, et al. Multi-omic characterization of allele-specific regulatory variation in hybrid pigs. Nat Commun. 2024;15(1):5587. https://doi.org/10.1038/s41467-024-49923-5.
34. Yuan C, Tang L, Lopdell T, Petrov VA, Oget-Ebrad C, Moreira GCM, et al. An organism-wide ATAC-seq peak catalog for the bovine and its use to identify regulatory variants. Genome Res. 2023;33:1848–64. https://doi.org/10.1101/gr.277947.123.
35. Liu C, Huang R, Jiang N, Zhou W, Liu Q, Du T, et al. Integration ATAC-Seq and RNA-Seq Analysis of Mammary Placodes in Erhualian and Bamaxiang Pigs Identified Candidate Genes Influencing Pig Teat Number Variation. Evol Appl. 2025;18:e70129. https://doi.org/10.1111/eva.70129.
36. Mao Y, Su C, Yang H, Ma X, Zhao F, Qu B, et al. PI3K/AKT/mTORC1 signalling pathway regulates MMP9 gene activation via transcription factor NF-κB in mammary epithelial cells of dairy cows. Anim Biotechnol. 2024;35:2314100. https://doi.org/10.1080/10495398.2024.2314100.
37. Chen H, Qiu D, Miao X, Yang W, He Q, Ren H, et al. Zearalenone Depresses Lactation Capacity Through the ROS-Mediated PI3K/AKT Pathway. Anim (Basel). 2025;15:1050. https://doi.org/10.3390/ani15071050.
38. Yang Y, Liu C, Zhang C, Xu Z, Zhang L, Cui Y, et al. Acetate Upregulates GPR43 Expression and Function via PI3K-AKT-SP1 Signaling in Mammary Epithelial Cells during Milk Fat Synthesis. J Agric Food Chem. 2023;71:16003–15. https://doi.org/10.1021/acs.jafc.3c00965.
39. Liu X, Robinson GW, Wagner KU, Garrett L, Wynshaw-Boris A, Hennighausen L. Stat5a is mandatory for adult mammary gland development and lactogenesis. Genes Dev. 1997;11:179–86. https://doi.org/10.1101/gad.11.2.179.
40. Tian M, Qi Y, Zhang X, Wu Z, Chen J, Chen F, et al. Regulation of the JAK2-STAT5 Pathway by Signaling Molecules in the Mammary Gland. Front Cell Dev Biol. 2020;8:604896. https://doi.org/10.3389/fcell.2020.604896.
41. Li L, Zhang Z, Li H, Zhou M, Li F, Chu C, et al. Research progress on the STAT signaling pathway in pregnancy and pregnancy-associated disorders. Front Immunol. 2023;14:1331964. https://doi.org/10.3389/fimmu.2023.1331964.
42. Cordero A, Pellegrini P, Sanz-Moreno A, Trinidad EM, Serra-Musach J, Deshpande C, et al. Rankl Impairs Lactogenic Differentiation Through Inhibition of the Prolactin/Stat5 Pathway at Midgestation. Stem Cells. 2016;34:1027–39. https://doi.org/10.1002/stem.2271.
43. Sundqvist A, Ten Dijke P, van Dam H. Key signaling nodes in mammary gland development and cancer: Smad signal integration in epithelial cell plasticity. Breast Cancer Res. 2012;14:204. https://doi.org/10.1186/bcr3066.
44. Ross S, Hill CS. How the Smads regulate transcription. Int J Biochem Cell Biol. 2008;40:383–408. https://doi.org/10.1016/j.biocel.2007.09.006.
45. Heldin C-H, Moustakas A. Role of Smads in TGFβ signaling. Cell Tissue Res. 2012;347:21–36. https://doi.org/10.1007/s00441-011-1190-x.
46. Ikushima H, Miyazono K. TGF-β signal transduction spreading to a wider field: a broad variety of mechanisms for context-dependent effects of TGF-β. Cell Tissue Res. 2012;347:37–49. https://doi.org/10.1007/s00441-011-1179-5.
47. Lee HK, Willi M, Wang C, Yang CM, Smith HE, Liu C, et al. Functional assessment of CTCF sites at cytokine-sensing mammary enhancers using CRISPR/Cas9 gene editing in mice. Nucleic Acids Res. 2017;45:4606–18. https://doi.org/10.1093/nar/gkx185.
48. Lee HK, Willi M, Liu C, Hennighausen L. Cell-specific and shared regulatory elements control a multigene locus active in mammary and salivary glands. Nat Commun. 2023;14:4992. https://doi.org/10.1038/s41467-023-40712-0.
49. Luk IY, Reehorst CM, Mariadason JM. ELF3, ELF5, EHF and SPDEF Transcription Factors in Tissue Homeostasis and Cancer. Molecules. 2018;23:2191. https://doi.org/10.3390/molecules23092191.
50. Howe LR, Subbaramaiah K, Kent CV, Zhou XK, Chang S-H, Hla T, et al. Genetic deletion of microsomal prostaglandin E synthase-1 suppresses mouse

mammary tumor growth and angiogenesis. Prostaglandins Other Lipid Mediat. 2013;106:99–105. https://doi.org/10.1016/j.prostaglandins.2013.04.002.
51. Chandrasekharan S, Foley NA, Jania L, Clark P, Audoly LP, Koller BH. Coupling of COX-1 to mPGES1 for prostaglandin E2 biosynthesis in the murine mammary gland. J Lipid Res. 2005;46:2636–48. https://doi.org/10.1194/jlr.M500213-JLR200.
52. Chang S-H, Liu CH, Conway R, Han DK, Nithipatikom K, Trifan OC, et al. Role of prostaglandin E2-dependent angiogenic switch in cyclooxygenase 2-induced breast cancer progression. Proc Natl Acad Sci U S A. 2004;101:591–6. https://doi.org/10.1073/pnas.2535911100.
53. Quang CT, Leboucher S, Passaro D, Fuhrmann L, Nourieh M, Vincent-Salomon A, et al. The calcineurin/NFAT pathway is activated in diagnostic breast cancer cases and is essential to survival and metastasis of mammary cancer cells. Cell Death Dis. 2015;6:e1658. https://doi.org/10.1038/cddis.2015.14.
54. McNeil M, Han Y, Sun P, Watanabe K, Jiang J, Chen N, et al. Nfatc1's Role in Mammary Epithelial Morphogenesis and Basal Stem/progenitor Cell Self-renewal. J Mammary Gland Biol Neoplasia. 2021;26:357–65. https://doi.org/10.1007/s10911-021-09502-6.
55. Zhong Q-H, Zha S-W, Lau ATY, Xu Y-M. Recent knowledge of NFATc4 in oncogenesis and cancer prognosis. Cancer Cell Int. 2022;22:212. https://doi.org/10.1186/s12935-022-02619-6.
56. Smalley MJ, Iravani M, Leao M, Grigoriadis A, Kendrick H, Dexter T, et al. Regulator of G-protein signalling 2 mRNA is differentially expressed in mammary epithelial subpopulations and over-expressed in the majority of breast cancers. Breast Cancer Res. 2007;9:R85. https://doi.org/10.1186/bcr1834.
57. Jurek B, Neumann ID. The Oxytocin Receptor: From Intracellular Signaling to Behavior. Physiol Rev. 2018;98:1805–908. https://doi.org/10.1152/physrev.00031.2017.
58. Vallone SA, García Solá M, Schere-Levy C, Meiss RP, Hermida GN, Chodosh LA, et al. Aberrant RET expression affects normal mammary gland post-lactation transition, enhancing cancer potential. Dis Model Mech. 2022;15:dmm049286. https://doi.org/10.1242/dmm.049286.
59. Pecar G, Liu S, Hooda J, Atkinson JM, Oesterreich S, Lee AV. RET signaling in breast cancer therapeutic resistance and metastasis. Breast Cancer Res. 2023;25:26. https://doi.org/10.1186/s13058-023-01622-7.

Publisher's note